Journal of Spinal Disorders
Vol. 7, No. 2, pp 93–101

Kinematics of the Cervical Spine Canal: Changes with Sagittal Plane Loads

*Ih-Hsin Chen, Anita Vasavada, and Manohar M. Panjabi

*Biomechanics Laboratory, Department of Orthopaedics and Rehabilitation, Yale University School of Medicine, New Haven, Connecticut, U.S.A., and *Division of Neurosurgery, Neurological Institute, Veterans General Hospital, Taipei, Taiwan, Republic of China*

Summary: Spondylotic myelopathy is a result of decreased spinal canal space due to degeneration. The space also may change with physiological movements. The knowledge of the normal physiological changes is necessary for a better understanding of the clinical symptoms. Using a novel technique, we measured the changes in disk bulge, ligamentum flavum bulge, and anteroposterior canal diameter in response to tension–compression forces (up to 40 N each) and combined loading: 2 Nm of flexion or extension moment combined with 20 N compression force in five human cadaveric lower cervical spine specimens (C4–C7). From tension to compression, the average disk bulge changed 1.13 mm or 10.1% of the original canal diameter. The ligamentum flavum bulge changed 0.73 mm or 6.5% of the canal diameter. From flexion to extension the average disk bulb changed 1.16 mm or 10.8% of the canal diameter, whereas the ligamentum flavum bulge changed 2.68 mm or 24.3% of the canal diameter. Most of the changes in the bulges occurred with a small load application around the neutral position of the spine. The results of this study demonstrate that ligamentum flavum bulge can contribute significantly to canal encroachment in extension and that a flexed posture increases the sagittal diameter of the spinal canal. **Key Words:** Disk bulge—Ligamentum flavum bulge—Load-displacement curves—Sagittal diameter—Canal kinematics.

Myelographic investigations have shown that the sagittal diameter of the lower cervical spinal canal decreases during extension of the neck (1,9,11), most probably due to the bulging of the ligamentum flavum (LF) (18,22). Ordinarily the inherent elasticity and pretension of the LF prevent its impingement on the spinal cord. However, hypertrophy, scarring of the LF, or loss of elasticity through degeneration might permit narrowing of the canal or spinal cord impingement during extension of the neck (7). Other factors that can contribute to canal encroachment include disk bulging and increase in the cord diameter on extension (22) and bony factors such as spondylotic bars, pincers phenomenon (23), and the relatively high incidence of retrolisthesis in elderly patients (19). This is particularly evident in those with a congenitally narrowed canal (5). Studies on human and cadaveric spines reporting mechanical response to loads have focused mainly on the spinal column. To our knowledge, no study has documented with precision the in situ kinematic characteristics of the disk and LF of the lower cervical spinal canal.

The objective in this in vitro study was to measure

Address correspondence and reprint requests to Manohar M. Panjabi, Department of Orthopaedics and Rehabilitation, Yale University School of Medicine, P.O. Box 208071, New Haven, CT 06520-8071, U.S.A.

the load–bulge characteristics of the disk and LF due to the application of tension–compression forces and complex loads of flexion–extension moments with compression force. Additionally, canal diameter changes were computed for the same loading conditions.

MATERIALS AND METHODS

Preparation of Specimens

Five intact human cadaveric cervical spines (C4–C7) were harvested fresh and stored at −20°C. The specimens (all male) ranged in age from 46 to 66 years (average 54). The ages of two specimens were unknown. Neither cause-of-death records nor roentgenographs showed any abnormalities beyond the normal degenerative changes.

The spines were dissected of all nonligamentous soft tissue, and the contents within the spinal canal were removed. The specimens were mounted symmetrically so that the midplan of the C5–C6 disc were horizontal to the testing apparatus (Fig. 1). Partial hemilaminectomy was performed over C5 and C6 to create a window, leaving facet joints intact. Through this window, 12 steel beads (0.8 mm in diameter) were attached with cyanoacrylic glue at intervals of ~1 mm mid-sagittally along both the posterior longitudinal ligament (PLL) and the LF. The seventh bead from the top, on both the PLL and LF, was glued onto the most protruding point of each ligament when the spine was put in extension. The centers of the beads acted as roentgenographic markers on lateral radiographs.

Testing Procedure

The specimens were tested in a high humidity environment. A heavy Plexiglas bar rigidly attached to the top of the specimen mounting was used both to facilitate load application and to constrain the movements of the specimens to the sagittal plane. Four types of loads were applied individually and incrementally. Lateral radiographs were taken after 30 s of load application to minimize the effects of creep.

To study the disk and LF bulges in response to axial loads, we applied 10 different forces: +40, +30, +20, +10, 0, −5, −10, −20, −30, and −40 N. (A positive force is tension or distraction, whereas a negative force is compression.) All axial forces were applied over the balance point of the specimen, defined as the point at which the resulting deformation was pure axial translation, with no flexion or extension rotation (i.e., the Plexiglas bar remained horizontal during the force applications).

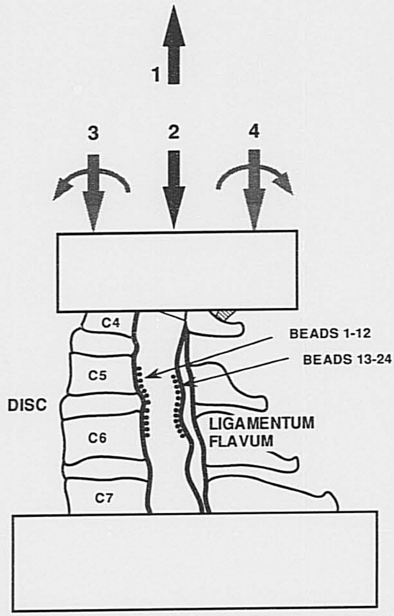

FIG. 1. Conceptual diagram of forces and moments applied to the specimen: 1, distraction force; 2, compression force; 3, flexion moment and compression force; 4, extension moment and compression force.

The following procedure was adopted to study the response to various moments. First, we applied a 20-N weight on the top mounting of the specimen to locate the balance point. Then, different combinations of the 20-N weight were applied on either side 10 cm from the balance point (i.e., 0–20, 5–15, 7.5–12.5, 10–10, 12.5–7.5, 15–5, and 20–0 N), resulting in seven corresponding moments, from 2 Nm flexion to 2 Nm extension. For the purpose of convenience, we have termed these loads as moments, although in reality they are complex: a combination of a moment and 20-N compressive force.

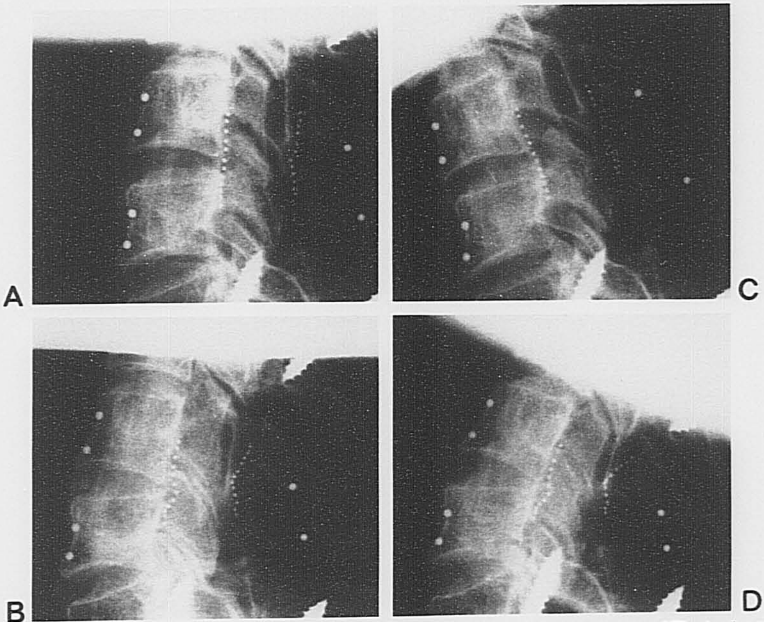

FIG. 2. Lateral radiographs of the specimen under **(A)** tension force, **(B)** compression force, **(C)** flexion moment, and **(D)** extension moment. Beads along PLL and LF act as roentgenological markers.

Digitization and Data Analysis

All radiographic markers shown on the lateral radiographs (Fig. 2) were digitized with an Altek digitizer (ACT22, Altek Corp., Silver Spring, MD) connected to a personal computer to calculate the magnitude of disk and LF bulges.

Disk and LF bulges were defined as the perpendicular distance from the corresponding most protruding bead (bead 7 for disk and bead 19 for LF) to a line connecting the two nearest beads attached to the edges of the adjacent vertebrae. The disk bulge and LF bulge are shown in Fig. 3.

Sagittal canal diameters were obtained by calculating the distance between bead pairs along the PLL and LF, including the diameter of the bead. All possible combinations of bead pairs (from beads 1 through 12 on the PLL, to beads 13 through 24 on the LF) were considered. Because there were 12 beads on each side of the canal, the total number of possible bead pair combinations was 144. The absolute minimum value of these 144 diameters represented the minimum canal diameter.

Repeatability of Measurement

The repeatability of the measurement method was ascertained by repeatedly digitizing on one radiograph each of the 24 radiographic markers 10 times and calculating the distance between the 12 marker pairs. The average standard deviation of the 12 calculated canal diameters was 0.04 mm; thus, the maximum error of the measurement method was 0.08 mm.

RESULTS

Load–bulge curves were plotted for the disk and LF in response to the compression–tension and flexion–

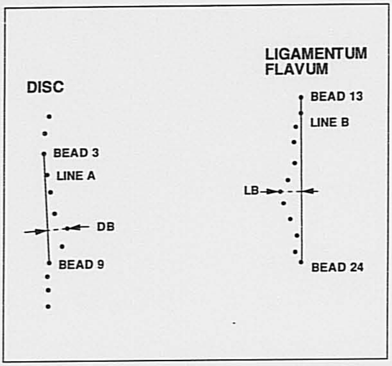

FIG. 3. Schematic of the beads along the posterior border of the disk and the LF. Line A connects beads 3 and 9, which define the edges of the two vertebrae; line B connects beads 13 and 24. DB and LB indicate the magnitude of the disk bulge and LF bulge, respectively.

extension loads. Although the initial zero-load bulge values were different for each specimen, we have centered all of the curves around zero. Thus, the values presented in Figs. 4–7 represent the change in disk or

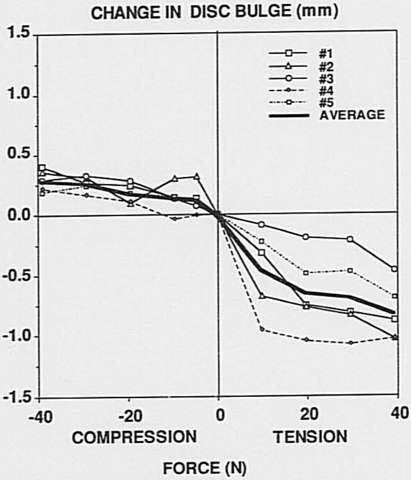

FIG. 4. Change in disk bulge versus tension-compression force.

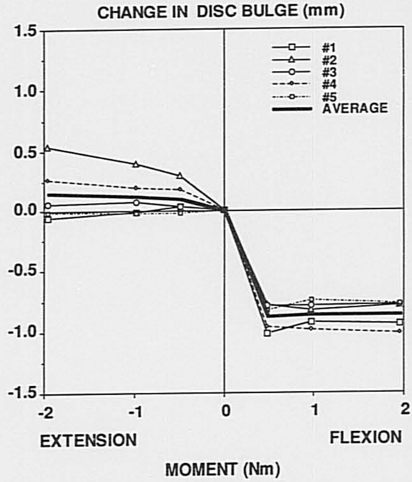

FIG. 5. Change in disk bulge versus flexion–extension moments.

ligamentous bulge. The averages and standard deviations of the maximum disk and ligament bulges and minimum canal diameter measurements are presented in Tables 1–3.

Disk Bulge

Tension–Compression (Fig. 4, Table 1)

The force–bulge curves were sigmoidal in shape; that is, the maximum change of the disk bulge took place in response to small tensile and compressive forces. The average disk bulge at zero load was 0.91 mm, increasing to 1.21 mm with compression and decreasing to 0.08 mm with tension. The average change in the canal diameter due to disk bulge, from tension to compression, was 1.13 mm or a decrease of 10.1% of the average unloaded canal diameter.

Flexion–Extension (Fig. 5, Table 1)

The moment–bulge curves were also sigmoidal in character. The average disk bulge at zero load was 1.00 mm, which increased to 1.24 mm with extension and decreased to 0.08 mm with flexion. The average change in the canal diameter was 1.16 mm, a decrease

of 10.8%, with the spine going from flexion to extension.

LF Bulge

Tension–Compression (Fig. 6, Table 2)

The average LF bulge was 1.09 mm at zero load, which increased to 1.56 mm with compression and decreased to 0.84 mm with tension. The average decrease in the spinal canal diameter, from tension to compression, was 0.73 mm or 6.5%.

Flexion–Extension (Fig. 7, Table 2)

The LF bulges in response to flexion and extension moments were markedly sigmoidal. The average LF bulge at zero moment was 1.14 mm, which increased with spinal extension to 2.70 mm and decreased with flexion to 0.02 mm. The average decrease, from flexion to extension, in the canal diameter was 2.68 mm, a change of 24.3% of the unloaded canal diameter.

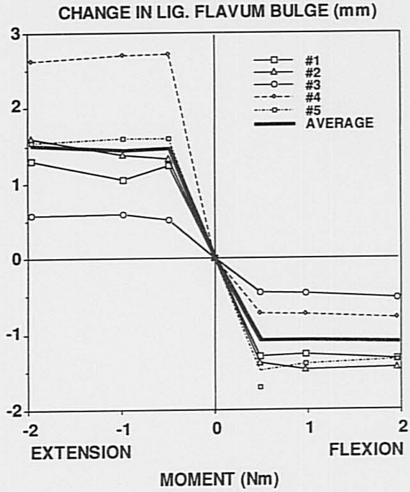

FIG. 7. Change in LF bulge versus flexion–extension moments.

Canal Diameter

Tension–Compression (Fig. 8, Table 3)

The average minimum canal diameter under zero load was 11.12 mm. Under compression, the minimum diameter decreased to 10.42 mm. With distraction, the minimum diameter was 12.03 mm, resulting in a net change of 1.62 mm, or 14.5% of the original diameter.

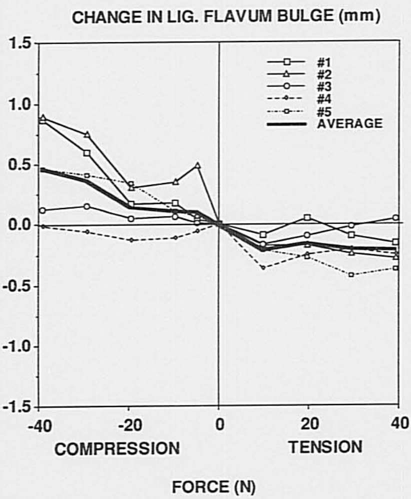

FIG. 6. Change in LF bulge versus tension–compression force.

Flexion–Extension (Fig. 8, Table 3)

With no applied moment, the average minimum canal diameter was 10.83 mm. An applied extension moment decreased the average minimum canal diameter to 9.74 mm, whereas an applied flexion moment increased the diameter to 12.58 mm. The total decrease in minimum canal diameter from flexion to extension was 2.84 mm, or 26.2%.

DISCUSSION

Under axial forces, the total changes in the LF bulge from compression to distraction were on average 70% of the changes of the disk bulge, which were all close to 1 mm. In response to the moments, however, the average change in LF bulge was 2–3 mm, usually more than twice the magnitude of the disk bulge. LF bulges showed more variation among specimens, perhaps corresponding to the degree of relative degeneration. Our observation of greater change in

TABLE 1. *Disk bulge data*

	Specimen 1	2	3	4	5	Average ± SD
Axial forces						
No load						
Canal diameter	11.42	10.81	9.46	11.57	12.33	11.12 ± 1.07
Bulge	0.88	1.34	0.62	1.00	0.69	0.91 ± 0.29
Tension of 40 N						
Bulge	0.00	0.30	0.15	−0.04	0.00	0.08 ± 0.14
Change in bulge	−0.89	−1.05	−0.47	−1.04	−0.70	−0.83 ± 0.25
Change as % of canal diameter	−7.8	−9.7	−5.0	−9.0	−5.6	−7.4 ± 2.0
Compression of 40 N						
Bulge	1.29	1.70	0.90	1.22	0.93	1.21 ± 0.32
Change in bulge	0.41	0.36	0.28	0.22	0.24	0.30 ± 0.08
Change as % of canal diameter	3.6	3.3	3.0	1.9	1.9	2.7 ± 0.8
Tension to compression						
Change in bulge	1.30	1.40	0.75	1.25	0.94	1.13 ± 0.27
Change as % of canal diameter	11.3	13.0	7.9	10.8	7.6	10.1 ± 2.3
Sagittal moments						
No load						
Canal diameter	11.23	10.59	8.98	11.51	11.83	10.83 ± 1.13
Bulge	1.07	1.05	0.89	1.11	0.87	1.00 ± 0.11
Flexion of 2 Nm						
Bulge	0.06	0.22	−0.03	0.10	0.05	0.08 ± 0.09
Change in Bulge	−1.01	−0.83	−0.92	−1.01	−0.83	−0.92 ± 0.09
Change as % of canal diameter	−9.0	−7.8	−10.2	−8.8	−7.0	−8.6 ± 1.2
Extension of 2 Nm						
Bulge	1.20	1.59	0.96	1.37	1.09	1.24 ± 0.24
Change in Bulge	0.13	0.54	0.07	0.26	0.21	0.24 ± 0.18
Change as % of canal diameter	1.1	5.1	0.8	2.3	1.8	2.2 ± 1.7
Flexion to extension						
Change in Bulge	1.14	1.37	0.99	1.27	1.04	1.16 ± 0.16
Change as % of canal diameter	10.1	12.9	11.0	11.1	8.8	10.8 ± 1.5

Values are expressed in millimeters, except where otherwise indicated.

the LF bulge as compared with the disk bulge, in response to the flexion–extension moments, supports the previous belief from in vivo studies that the LF bulging is the major contributing factor to the dynamic encroachment of the cervical spinal canal (18,22).

Under axial compressive forces, canal diameter decreased by 0.7 mm on average, whereas distraction produced an average 0.9-mm increase in diameter. A combination of compression and extension resulted in an average decrease of 1.1 mm in the canal diameter. All of these changes were <10% of the original minimum canal diameter, which averaged ~11 mm. However, compression with flexion yielded the largest change in canal diameter, on average 1.75 mm, or an increase of 16% over the neutral canal diameter.

The patterns of load–bulge curves of disk and LF are worth discussing. For example, both the disk and LF bulge versus flexion–extension moment formed a sigmoidal curve, similar to the load-displacement curve of a cervical spine specimen (15). Similar to the cervical spine, there is a significant change in the bulge in the vicinity of the neutral position of the spinal column. By definition, the neutral zone is that region within the range of motion in which the spine can be displaced with the application of a very small load (14). The neutral zone is spread around the neutral position of the spine. The sigmoidal shape of the load–bulge curves of the disk and LF thus reflects the neutral zone of the spine. In three-dimensional studies of the cervical spine specimens, the sigmoidal shape of the load-displacement curve has been observed in response to all physiological loads, i.e., lateral bendings and axial rotations, in addition to flexion and extension. Although no measurements have been made of the disk and LF bulges to these nonsagittal plane loads, one may expect similar qualitative results.

The spinal canal of the cervical spine has been measured both in vivo and in vitro by several investigators using direct measurement (13), lateral radiographs (4,5,23) and computed tomography scans (10). The

TABLE 2. *Ligamentum flavum bulge data*

	Specimen					
	1	2	3	4	5	Average ± SD
Axial forces						
No load						
Canal diameter	11.42	10.81	9.46	11.57	12.33	11.12 ± 1.07
Bulge	0.99	1.52	1.13	0.70	1.11	1.09 ± 0.29
Tension of 40 N						
Bulge	0.84	1.24	0.97	0.45	0.68	0.84 ± 0.30
Change in bulge	−0.16	−0.28	−0.16	−0.25	−0.42	−0.25 ± 0.11
Change as % of canal diameter	−1.4	−2.6	−1.7	−2.2	−3.4	−2.2 ± 0.8
Compression of 40 N						
Bulge	1.86	2.41	1.29	0.68	1.57	1.56 ± 0.65
Change in bulge	0.87	0.90	0.15	−0.02	0.46	0.47 ± 0.41
Change as % of canal diameter	7.6	8.3	1.6	−0.1	3.8	4.2 ± 3.7
Tension of compression						
Change in bulge	1.03	1.17	0.32	0.23	0.89	0.73 ± 0.43
Change as % of canal diameter	9.0	10.9	3.3	2.0	7.2	6.5 ± 3.7
Sagittal moments						
No load						
Canal diameter	11.23	10.59	8.98	11.51	11.83	10.83 ± 1.13
Bulge	1.16	1.82	1.04	0.57	1.10	1.14 ± 0.45
Flexion of 2 Nm						
Bulge	−0.17	0.35	0.50	−0.22	−0.38	0.02 ± 0.38
Change in bulge	−1.33	−1.47	−0.54	−0.79	−1.48	−1.12 ± 0.43
Change as % of canal diameter	−11.8	−13.9	−6.0	−6.9	−12.5	−10.2 ± 3.5
Extension of 2 Nm						
Bulge	2.47	3.41	1.62	3.19	2.81	2.70 ± 0.70
Change in bulge	1.31	1.59	0.58	2.62	1.71	1.56 ± 0.73
Change as % of canal diameter	11.7	15.0	6.5	22.7	14.5	14.1 ± 5.9
Flexion to extension						
Change in bulge	2.64	3.06	1.12	3.41	3.19	2.68 ± 0.92
Change as % of canal diameter	23.5	28.9	12.5	29.6	27.0	24.3 ± 7.0

Values are expressed in millimeters, except where otherwise indicated.

kinematics of the canal, on the other hand, have been measured by few. Using myelography, Penning and van der Zwaag measured the subarachnoidal space in three postures (20), and obtained the average values as 12.5 mm for neutral, 11 mm for extension, and 13 mm for flexion posture. There is a good agreement between these and our results (corresponding values are 10.8, 9.7, and 12.6 mm), especially considering the limited resolution (we estimate ±0.5 mm) of this 28-year-old study.

There are not many studies in which the kinematics of the cervical spinal canal have been studied. LF bulge in the cervical spine was measured by Jia et al. (6). They measured functional changes of the LF in full extension and flexion using cervical spine specimens that were cut in the midsagittal plane. They concluded that the LF became thickened, shortened, and protruded about 3.5 mm into the canal at the C5–C6 level in hyperextension. These values are more than twice the change in LF bulge measured in our study. We believe these large changes result from complete cutting of the specimen in the mid-sagittal plane, thus determining the anatomic integrity of the spine. Our hemilaminectomy model, preserving the disk, facet joints, and most of the LF, is more physiological.

Disk bulge has been measured in the lumbar spine, but not in the cervical spine. However, it may be of interest to compare the cervical disk bulge (our study) to that in the lumbar spine in the earlier studies. Brown et al. measured the lumbar disk bulge in cadaveric specimens without the posterior elements (3). For 6° of extension rotation, they measured an average posterior disk bulge of 1.5 mm. This is slightly more than the corresponding cervical spine value of 1.24 mm. Disk bulge change in the lumbar spine due to compression is much smaller. It has been measured to be ~0.2 mm for 1,000 N load (2). In another study, posterior disk bulge was measured in response to 800 N compression and additional 9.8 Nm extension moment (21). The results were 0.34 mm and 0.58 mm, respectively. Our corresponding cervical spine results

TABLE 3. *Minimum canal diameter data*

	Specimen 1	Specimen 2	Specimen 3	Specimen 4	Specimen 5	Average ± SD
Axial forces						
No load						
Canal diameter	11.42	10.81	9.46	11.57	12.33	11.12 ± 1.07
Tension of 40 N						
Canal diameter	12.51	11.99	9.71	12.69	13.28	12.03 ± 1.38
Change in diameter	1.09	1.18	0.25	1.12	0.95	0.92 ± 0.38
Change in diameter (%)	9.6	10.9	2.6	9.7	7.7	8.1 ± 3.3
Compression of 40 N						
Canal diameter	10.60	9.46	8.88	11.41	11.72	10.42 ± 1.22
Change in diameter	−0.82	−1.35	−0.58	−0.16	−0.61	−0.70 ± 0.43
Change in diameter (%)	−7.2	−12.5	−6.1	−1.4	−4.9	−6.4 ± 4.0
Tension to compression						
Change in diameter	1.91	2.52	0.82	1.28	1.55	1.62 ± 0.64
Change in diameter (%)	16.8	23.4	8.7	11.0	12.6	14.5 ± 5.8
Sagittal moments						
No load						
Canal diameter	11.23	10.59	8.98	11.51	11.83	10.83 ± 1.13
Flexion of 2 Nm						
Canal diameter	13.39	12.65	10.38	12.78	13.72	12.58 ± 1.30
Change in diameter	2.15	2.06	1.40	1.27	1.89	1.75 ± 0.40
Change in diameter (%)	19.2	19.4	15.6	11.0	16.0	16.2 ± 3.4
Extension of 2 Nm						
Canal diameter	10.45	8.85	8.39	9.91	11.11	9.74 ± 1.12
Change in diameter	−0.78	−1.74	−0.59	−1.60	−0.72	−1.09 ± 0.54
Change in diameter (%)	−6.9	−16.4	−6.6	−13.9	−6.1	−10.0 ± 4.8
Flexion to extension						
Change in diameter	2.93	3.80	1.99	2.87	2.61	2.84 ± 0.65
Change in diameter (%)	26.1	35.8	22.2	25.0	22.1	26.2 ± 5.7

Positive values indicate increases in canal diameter, negative values indicate decreases in diameter. Values are expressed in millimeters, except where otherwise indicated.

were 0.30 mm and 0.54 mm, respectively, for the loads of 60 N compression and 2 Nm additional extension moment. Thus, the results seem to be similar for the cervical and lumbar regions. Of course, the exact loads in vivo are not known, and the experimental loads are only estimates.

It has been established that the ratio of the cord to subarachnoid space is greatest at the levels from C5 through C7, where the clinical consequences of compressive change are most significant (12,17,19). This is the reason behind our choice of the C5–C6 level for the study of load–bulge curves of the disk and the LF. Panjabi et al. (16) showed that cervical spine kinematics are not altered by cutting all posterior elements, providing the facet joints remain intact. Reuber et al. found that the posterior element removal in the lumbar spine did not affect disk bulge significantly (21). Thus, the hemilaminectomy for inserting beads into the canal used in the present study is justified.

Our study is an in vitro model where muscle forces are not present. Thus, the effect of muscles could not be assessed. However, there are certain advantages to an in vitro experiment in comparison with in vivo studies. In general, the accuracy of measurement is significantly higher, which is important when the changes to be measured are small. Our repeatability, measured as a standard deviation of the spinal canal diameter measured repeatedly, was 0.04 mm, thus giving a maximum error of 0.08 mm. Because the changes in the bulges due to the loads applied are in the vicinity of 1 mm, the need for the high repeatability is well justified.

The present investigation has provided a new method to measure disk bulges and LF bulges under forces and moments. Not only is the accuracy of our method significantly better than were the previous methods, but the kinematic characteristics of the disk and LF bulges are clearly elucidated by means of the load–bulge curves. This experimental study validated the clinical understanding that LF bulging is a major contributing factor to the encroachment of the cervical spinal canal. Furthermore, our study demon-

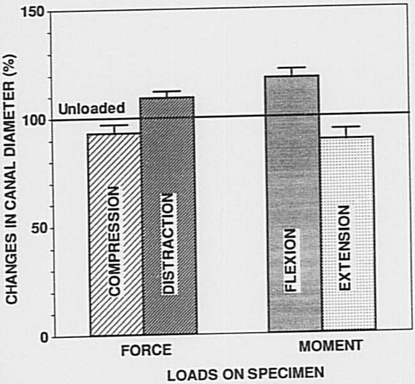

FIG. 8. Average sagittal canal diameter changes in response to external loads.

strated that a flexed posture increases the spinal canal diameter. Conversely, extension produces the narrowest spinal canal.

Acknowledgment: Support was provided in part by National Institutes of Health Grant AR39209 and Center for Environmental Health and Injury Control Grant R49-CCR103551.

REFERENCES

1. Bracham J, Herzberger E: Cervical spondylosis and compression of spinal cord. *JAMA* 161:1560, 1956
2. Brinckmann P, Horst M: The influence of vertebral body fracture, intradiscal injection, and partial discectomy on the radial bulge and height of human lumbar discs. *Spine* 10:138, 1985
3. Brown T, Hansen RJ, Yorra AJ: Some mechanical tests on the lumbosacral spines with particular reference to the intervertebral disc: a preliminary report. *J Bone Joint Surg* [*Am*] 39:1135, 1957
4. Eismont FJ, Clifford S, Goldberg M, Green B: Cervical sagittal spinal canal size in spine injury. *Spine* 9:663–666, 1984
5. Epstein JA, Carras R, Hyman RA, Costa S: Cervical myelopathy caused by developmental stenosis of the spinal canal. *J Neurosurg* 51:362–367, 1979
6. Jia L, Shen Q, Chen D, Zhang W: Dynamic changes of the cervical ligamentum flavum in hyperextension–hyperflexion movement and their measurement. *Chin Med J* 103:66–70, 1990
7. Johnson RM, Crelin ES, White AA, Panjabi MM: Some new observations on the functional anatomy of the lower cervical spine. *Clin Orthop* 111:192–200, 1975
8. Kambin P: Bulging annulus. *Orthop Trans* 2:23, 1987
9. Kaplan L, Kennedy F: Effect of head position on manometrics of cervical spinal fluid in cervical regions: new diagnostic test. *Brain* 73:337, 1950
10. Matsuura P, Waters R, Adkins RH, Rothman S, Gurbani N, Sie I: Comparison of computerized tomography parameters of the cervical spine in normal control subjects and spinal cord–injured patients. *J Bone Joint Surg* [*Am*] 71:183–188, 1989
11. Nugont GR: Clinical pathological correlations in cervical spondylosis. *Neurology* 9:273, 1959
12. Ogino H, Tada K, Okada K, Yonenobu K, Yamamoto T, Ono K, Namiki H: Canal diameter, anteroposterior compression ratio, and spondylotic myelopathy of the cervical spine. *Spine* 8:1–15, 1983
13. Panjabi MM, Duranceau J, Goel V, Oxland T, Takata K: Cervical human vertebrae: quantitative three-dimensional anatomy of the middle and lower regions. *Spine* 16:861–869, 1991
14. Panjabi MM, Goel VK, Takata K: Physiologic strains in the lumbar spinal ligaments: an *in vitro* biomechanical study. *Spine* 7:192–202, 1982
15. Panjabi MM, Summers DJ, Pelker R, Videman T, Friedlaender GE, Southwick WO: Three-dimensional load-displacement curves due to forces on the cervical spine. *J Orthop Res* 4:152–161, 1986
16. Panjabi MM, White AA, Johnson RM: Cervical spine mechanics as a function of transection of components. *J Biomech* 8:327–336, 1975
17. Parke WW: Correlative anatomy of cervical spondylotic myelopathy. *Spine* 13:831–837, 1988
18. Payne EE, Spillane JD: The cervical spine: an anatomical study of 70 specimens with special reference to the problem of cervical spondylosis. *Brain* 80:571, 1957
19. Penning L: Some aspect of plain radiology of the cervical spine in chronic myelopathy. *Neurology* 12:513–519, 1962
20. Penning L, van der Zwaag P: Biomechanical aspects of spondylotic myelopathy. *Acta Radiol* 5:1090, 1966
21. Reuber M, Schultz A, Denis F, Spencer D: Bulging of lumbar intervertebral disks. *J Biomech Eng* 104:187, 1982
22. Tayler AR: Mechanism and treatment of spinal cord disorders associated with cervical spondylosis. *Lancet* 1:717, 1953
23. Wolf BS, Khilnan M, Malis L: The sagittal diameter of the bony cervical spinal canal and its significance in cervical spondylosis. *J Mt Sinai Hosp* 23:283, 1956